Single Channel Properties and Regulated Expression of Ca^{2+} Release-Activated Ca^{2+} (CRAC) Channels in Human T Cells

Alla F. Fomina, Christopher M. Fanger, J. Ashot Kozak, and Michael D. Cahalan

Department of Physiology and Biophysics, University of California Irvine, Irvine, California 92697-4561

Abstract. Although the crucial role of Ca^{2+} influx in lymphocyte activation has been well documented, little is known about the properties or expression levels of Ca^{2+} channels in normal human T lymphocytes. The use of Na^+ as the permeant ion in divalent-free solution permitted Ca^{2+} release-activated Ca^{2+} (CRAC) channel activation, kinetic properties, and functional expression levels to be investigated with single channel resolution in resting and phytohemagglutinin (PHA)-activated human T cells. Passive Ca^{2+} store depletion resulted in the opening of 41-pS CRAC channels characterized by high open probabilities, voltage-dependent block by extracellular Ca^{2+} in the micromolar range, selective Ca^{2+} permeation in the millimolar range, and inactivation that depended upon intracellular Mg^{2+} ions. The number of CRAC channels per cell increased greatly from

$\sim$15 in resting T cells to $\sim$140 in activated T cells. Treatment with the phorbol ester PMA also increased CRAC channel expression to $\sim$60 channels per cell, whereas the immunosuppressive drug cyclosporin A (1 μM) suppressed the PHA-induced increase in functional channel expression. Capacitative Ca^{2+} influx induced by thapsigargin was also significantly enhanced in activated T cells. We conclude that a surprisingly low number of CRAC channels are sufficient to mediate Ca^{2+} influx in human resting T cells, and that the expression of CRAC channels increases $\sim$10-fold during activation, resulting in enhanced Ca^{2+} signaling.

Key words: T lymphocyte • Ca^{2+} channel • CRAC channel • T cell activation • Ca^{2+} signaling

Introduction

T lymphocytes play fundamental and diverse roles in the immune response including the recognition of antigens, secretion of cytokines, and killing of foreign or virus-infected cells. T cell receptor (TCR)[1] engagement by specific antigen/major histocompatibility complex proteins on an antigen-presenting cell initiates a program of intracellular signaling within the T cell. By cross-linking surface receptors, the mitogenic lectin phytohemagglutinin (PHA) mimics the early antigen evoked events in a heterogeneous population of resting T cells. A sustained or oscillatory rise in intracellular Ca^{2+} concentration ($[Ca^{2+}]_i$) following TCR engagement is required to drive many of the subsequent events of lymphocyte activation, including the activation of transcription factors, modulation of cytoskeletal elements and motility, production and release of cy-

tokines, and cell proliferation (Metcalfe et al., 1980; Crabtree, 1989; Crabtree and Clipstone, 1994; Negulescu et al., 1994, 1996; Rao, 1994). The rise in $[Ca^{2+}]_i$ results initially from IP_3-induced Ca^{2+} release from internal stores and is sustained by Ca^{2+} influx across the plasma membrane (Donnadieu et al., 1992; Hess et al., 1993; Dolmetsch and Lewis, 1994; Lewis and Cahalan, 1995; Lewis, 1999). In parallel with the Ca^{2+} signaling pathway, contact with an antigen-presenting cell triggers a PKC-dependent pathway leading to transcriptional activation of additional genes via the Fos/Jun transcription factor AP-1. The Ca^{2+} and PKC pathways interact at several levels, resulting in amplification of downstream signaling. The crucial role of Ca^{2+} for lymphocyte activation is underscored by clinical use of the immunosuppressive drug, cyclosporin A (CsA), which inhibits calcineurin, a $[Ca^{2+}]_i$-dependent phosphatase (Schreiber and Crabtree, 1992; Rao et al., 1997; Crabtree, 1999).

In Jurkat T cells dialyzed with a strong Ca^{2+} buffer or stimulated acutely with PHA, Ca^{2+} enters via Ca^{2+}-selective, store-operated channels (Lewis and Cahalan, 1989). These channels, also seen in mast cells and named Ca^{2+} release-activated Ca^{2+} (CRAC) channels, can be activated by treatment with thapsigargin (Tg) to inhibit Ca^{2+} pumps

---

located in the ER, thus bypassing proximal receptor signaling and IP$_3$ generation while depleting the Ca^{2+} store (Hoth and Penner, 1992; Zweifach and Lewis, 1993). The resulting Ca^{2+} influx through CRAC channels produces a sustained [Ca^{2+}]$_i$ signal that is capable of triggering gene expression (Negulescu et al., 1994; Fanger et al., 1995). CRAC channels are highly selective for Ca^{2+} under physiological conditions, but exhibit permeability to Na$^+$ and other monovalent cations when extracellular divalent ions are withdrawn, with a size cutoff for permeation of 6Å (Hoth and Penner, 1993; Lepple-Wienhues and Cahalan, 1996; Kerschbaum and Cahalan, 1998). Although the mechanism linking Ca^{2+} store depletion to the opening of CRAC channels remains elusive, progress has been made in characterizing CRAC channels at the single channel level, using Na$^+$ as a charge carrier to amplify the single channel conductance (Kerschbaum and Cahalan, 1999). Using this approach, single CRAC channels with 36–40-pS Na$^+$ conductance were observed in Jurkat T cells. The unitary CRAC channel phenotype provides a unique single channel signature for identifying CRAC channels in other cell types. Here, with single channel resolution during whole-cell recording, we describe the properties and regulated expression of CRAC channels in resting and activated T lymphocytes from human donors.

Materials and Methods

Cell Culture

T lymphocytes were purified from freshly drawn peripheral blood of healthy volunteers using a nylon-wool column and placed into culture in modified RPMI 1640 medium in a 5% CO$_2$ incubator at 37°C according to standard procedure (Hess et al., 1993). Purified human T cells (>90% CD3$^+$, containing CD4$^+$ and CD8$^+$ T cells) were pretreated in vitro with 4 μg/ml phytohemagglutinin P (PHA; Difco), 40 nM phorbol 12-myristate 13-acetate (PMA; Calbiochem), or 500 nM ionomycin (Calbiochem) for varying times; cells from the PHA-treated population are referred to as activated T cells. In some experiments, 0.1–1 μM CsA from a 1-mM stock solution in DMSO (Sigma-Aldrich) was added simultaneously with PHA to inhibit activation and proliferation. For electrophysiological and [Ca^{2+}]$_i$-imaging experiments, resting, activated, or PMA-treated T cells were placed on poly-L-lysine–coated glass coverslips and mounted on the stage of an inverted microscope.

Electrophysiology

Whole-cell recording was performed using an EPC-9 amplifier (HEKA). The resistance of sylgard-coated, fire-polished glass microelectrodes varied from 2 to 4 MΩ. Unless otherwise indicated, currents were sampled at 5 kHz and digitally filtered off-line at 1.4 kHz. After establishing the whole-cell recording configuration, cells were held at 0 mV and square pulses to −120 mV for 200 ms or ramp voltages from −120 to +50 mV were applied every 0.7 s. The short-pulse protocol was chosen to avoid the damaging effect of strong hyperpolarization on membrane integrity. In some experiments, long pulses (up to 2,500 ms duration) were applied to voltages ranging from −120 to −10 mV. Liquid junction potentials were measured for all internal and external solutions and corrections were made during data acquisition. All recordings were performed at room temperature (∼21°C). In some experiments, cells were pretreated with 2 μM Tg (Alexis Chemical) in Ringer solution for 15–45 min on the microscope stage. Cell capacitance (C_m) was monitored to determine the membrane surface area, based upon a specific C_m value of 1 μF/cm^2.

Solutions

CRAC channels were activated by passive Ca^{2+} store depletion with the Ca^{2+} chelator 1,2-bis(2-aminophenoxy)ethane-N,N,N′,N′-tetraacetic acid (BAPTA) included in the pipette solution. The standard internal solution was composed of 128 mM Cs–aspartate, 10 mM Cs–Hepes, 12 mM BAPTA, and 0.9 mM CaCl$_2$. In some experiments, either 3.2 mM Mg^{2+} or 30 μM IP$_3$ (Sigma-Aldrich) was added to standard solution. To detect single channel CRAC currents, the concentration of external divalent cations was lowered below 1 μM to enable Na$^+$ to permeate and serve as the charge carrier. The standard external solution contained 145 mM Na-methane sulfonate, 5 mM NaCl, 10 mM N-hydroxyethyl-ethylenediamine-triacetic acid (HEDTA), 10 mM Hepes, and 10 mM D-glucose. For some experiments, Na$^+$ was replaced with N-methyl-D-glucamine (NMDG$^+$). Ca^{2+} currents were detected in Ca^{2+}-containing solution: 155 mM Na-methane sulfonate, 5 mM NaCl, 2 mM Ca-methane sulfonate, 10 mM Hepes, and 10 mM D-glucose. Aliquots from Ca^{2+}-saturated HEDTA solution were added to standard solution to yield the desired concentration of extracellular free Ca^{2+} (1, 10, and 50 μM). The pH of all solutions was 7.2, and osmolarity was 300–305 mOsm. The HEDTA stock solution saturated with Ca^{2+} was prepared using a pH-metric method (Neher, 1988). Extracellular solutions and drugs were applied using a gravity-driven perfusion system with output tip diameter of ∼50 μm placed ∼50 μm from the cell. Five barrels were inserted close to the output tip, and solution exchange controlled manually by valves. A complete local solution exchange was achieved within 2 s. For [Ca^{2+}]$_i$ imaging, cells were bathed in normal Ringer solution consisting of 155 mM NaCl, 4.5 mM KCl, 1 mM MgCl$_2$, 2 mM CaCl$_2$, 10 mM D-glucose, 5 mM Hepes, pH 7.4. Ca^{2+}-free Ringer solution contained 1 mM EGTA in place of CaCl$_2$ and a total of 3 mM MgCl$_2$. Ca^{2+} concentration in normal Ringer solution was lowered to 300 μM to reduce the rate of capacitative Ca^{2+} influx in some measurements. In K$^+$ Ringer, KCl replaced NaCl.

[Ca^{2+}]$_i$ Imaging

Ca^{2+} imaging experiments were performed as described previously (Fanger et al., 2000). In brief, resting or PHA-activated T cells were incubated for 30 min at 21–24°C with 1 μM fura-2 acetoxymethyl ester (Molecular Probes) in medium. Cells were then washed, resuspended, adhered to poly-L-lysine–coated glass coverslips, and mounted in a chamber permitting rapid (∼1 s) solution exchange by a syringe-driven perfusion system. A Videoprobe Ca^{2+} imaging system (ETM Systems) was used for [Ca^{2+}]$_i$ measurement. Tg was used to deplete Ca^{2+} stores and elicit Ca^{2+} influx. Intracellular Ca^{2+} concentrations were calculated using the standard equation [Ca^{2+}]$_i$ = K^* (R − R_{min})/(R_{max} − R), where values of K^*, R_{min}, and R_{max}, determined by in vitro calibrations in a glass chamber, were adjusted to the anticipated in vivo values by correction factors derived from T cells dialyzed with known Ca^{2+} concentration standards (Molecular Probes) as described previously (Fanger et al., 2000).

Cytokine Assay

After 2 d of activation under various conditions, brefeldin A was added for 4–12 h. Cells were fixed, permeabilized, and IL-2 content assessed by staining with FITC–conjugated anti–human IL-2 antibody according to Cytofix/Cytoperm Plus kit instructions (BD PharMingen). Stained cells were analyzed using a FACScan™ (Becton Dickinson) and Cell QUEST™ software.

Data Analysis

Whole-cell currents were initially processed with PULSE™ analysis software (HEKA) and then exported to Microcal Origin 5.0 software (Microcal Software, Inc.) or TAC (Bruxton Corp.) for further analysis. Traces recorded before CRAC channel activation were used as a template for leak subtraction. Initial analyses of imaging data were performed using IGOR Pro software (WaveMetrics, Inc.) with home-written macros and extensions. Two population Student's t test and Mann-Whitney U test were employed for statistical analysis. Data were considered statistically significant at $P < 0.01$. All statistical data are reported as mean ± SEM, and n = the number of cells tested.

Results

### CRAC Channels in Resting and Activated Human T Cells

Fig. 1 shows inward Na$^+$ current through single CRAC

channels in a resting T cell. After patch rupture (break in) to initiate whole-cell recording, the first indication of channel activity was the appearance of very brief opening events, <1 ms in duration, within an average of 68 ± 12 s after break in ($n = 18$ cells; Fig. 1 A, top left trace). Brief openings were typically observed for ~1 min, and then the first open channel stabilized abruptly to a state characterized by long openings, short closed events, and high open probability ($P_o = 0.95$ at –120 mV). The average latency between break in and stable openings of the first channel was 116.4 ± 11.3 s ($n = 33$). Additional single channels opened sequentially, with an average time constant of activation (τ_{act}) of 85 ± 15 s ($n = 12$). Amplitude histograms during the activation phase showed equally spaced peaks of 4.8 ± 0.03 pA at -120 mV ($n = 23$), corresponding to a single channel chord conductance of 41 pS (Fig. 1 B). Fig. 1 C shows the time course of whole-cell current illustrating activation of a total of 16 channels in a resting T cell. The number of open channels gradually declined with a run-down time constant (τ_r) of 940 ± 430 s ($n = 12$). Single channel activity at the beginning of activation and at the end of run-down exhibited the same high P_o values and open and closed channel lifetimes (Fig. 1, A and D), indicating that changes in the number of open channels underlie both activation and run-down processes. As expected for a store-operated channel, IP$_3$ (30 μM in the pipette) significantly decreased the latency between break in and the onset of channel activation (29.8 ± 15.3 s, $n = 13$), without affecting the average total number of open channels (Fig. 1 E). In cells pretreated with Tg (2 μM in Ringer for 15–45 min), many channels were already open and current was observed immediately after break in, with an additional increase during prolonged recording (Fig. 1 E). These results indicate that single CRAC channels can be detected in human T cells using Na$^+$ as the permeant ion, permitting channel activation, kinetic properties, and functional expression levels to be investigated with single channel resolution. In resting T cells, the number of CRAC channels simultaneously open during whole cell recording ranged from 2 to 50 per cell.

CRAC channels in activated T cells opened in a similar sequential manner, with a shorter delay before observing the first channel activity in comparison to resting T cells. Channel opening and stabilization typically began within seconds after break in, followed by rapid activation of several channels. Discrete inward current steps of 4.8 pA at -120 mV were resolved at the beginning of the experiment, similar to those observed in resting T cells (Fig. 2, A and B). CRAC channels in activated T cells also exhibited very high open probabilities ($P_o = 0.95$ at -120 mV), and similar rates of macroscopic current activation ($\tau_{act} = 114 \pm 9$ s, $n = 24$; Fig. 2, C and D), followed by slow run-down ($\tau_r = 1940 \pm 490$ s, $n = 11$). Peak currents typically represented the summed activity of 50–500 CRAC channels, averaging tenfold higher than in resting T cells.

Ion Permeation and Divalent Block

Several features of ion permeation and divalent block demonstrate that the single channel activity reported here in human T cells is closely similar to CRAC channels described previously in Jurkat T cells (Lepple-Wienhues and
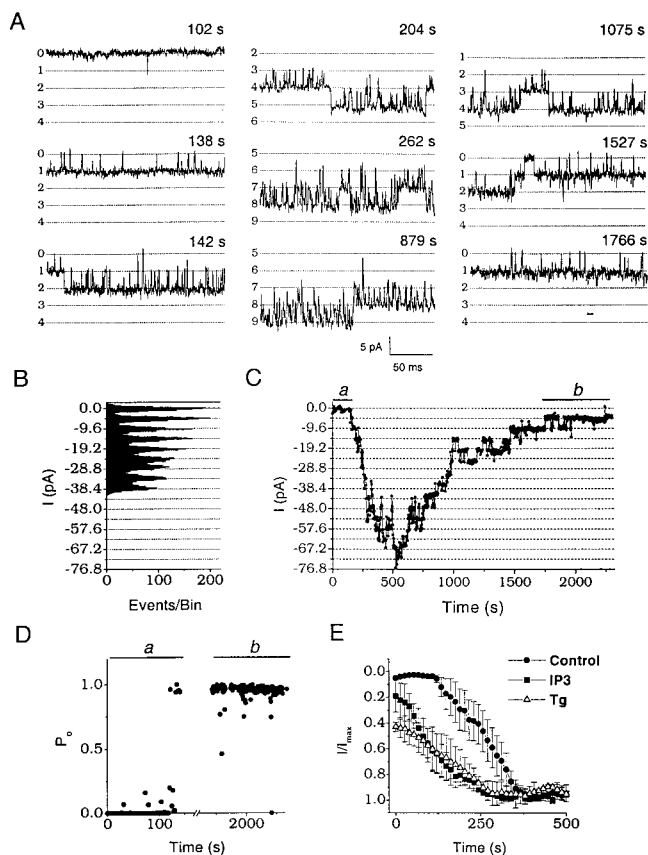

Figure 1. Na$^+$ current through CRAC channels in a resting T cell. All currents recorded in divalent-free solution using a Cs$^+$-aspartate pipette solution containing BAPTA with no Mg^{2+}. (A) Sequence of channel activation displaying currents at -120 mV at the indicated times following break in. Horizontal lines are multiples of 4.8 pA, with the number of open channels shown on the left. Please note baseline shifts in channel numbers for the middle and right columns. (B) All-points amplitude histogram (bin size = 0.2 pA) accumulated during nine consecutive current traces recorded at -120 mV, beginning 135 s after break in. Note that the histogram peaks are equally spaced with intervals of 4.8 pA, corresponding to the sequential and sustained opening of eight channels. (C) Time course of whole-cell current recorded from the same resting T cell. The current amplitude at each time point was measured off-line by averaging 5-ms intervals randomly selected within square-pulse traces. (D) Open probability (P_o) obtained from current traces with one channel active at the beginning of current activation (a) and after currents ran down to a single remaining active channel (b). a and b correspond to time intervals marked on C. P_o values were measured by integrating current traces containing one active channel. Missing points within the horizontal scale break represent skipped traces with more than one channel active. (E) Activation by passive store dialysis, IP$_3$, and Tg. Average time course of CRAC channel currents from representative resting T cells dialyzed with either normal BAPTA-containing pipette solution (Control, ●, $n = 4$), with 30 μM IP$_3$ added to the normal pipette solution (IP$_3$, ■, $n = 3$), or after preincubation with 2 μM Tg for 15–45 min (Tg, △, $n = 3$). All current traces were normalized to maximal current amplitude and then averaged.

Cahalan, 1996; Kerschbaum and Cahalan, 1998, 1999). Upon development of macroscopic Na$^+$ currents representing the activation of many CRAC channels, I–V curves rectified weakly and had a reversal potential of 0
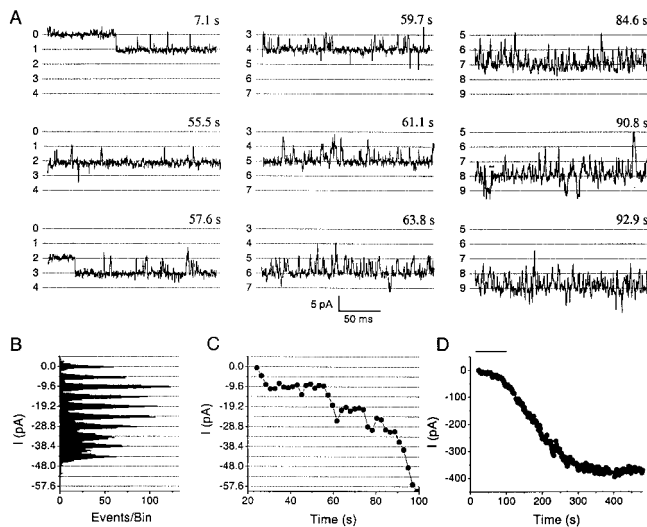
Figure 2. Na$^+$ currents through CRAC channels in an activated T cell. Same recording conditions as described in the legend to Fig. 1 A. (A) Sequence of channel activation at the indicated times. Horizontal lines are multiples of 4.8 pA, with the number of open channels shown on the left. Again, please note baseline shifts that indicate the number of open channels. (B) Amplitude histogram showing equally spaced peaks corresponding to the first nine channels that opened. (C and D) Time course of CRAC channel activation. C represents the initial time course marked with bar on D on an expanded time scale. Horizontal lines represent equally spaced intervals of 4.8 pA to illustrate the stepwise activation of channels.

mV (Fig. 3 A). Introduction of physiological levels of external Ca^{2+} resulted in much smaller macroscopic Ca^{2+} currents with more pronounced inward rectification and a positive reversal potential typical of I_{CRAC}. As expected for current through a common channel, Na$^+$ and Ca^{2+} current amplitudes in different cells were strongly correlated (Fig. 3 B), with a slope determined by linear regression of ~80, implying a much larger single channel conductance for Na$^+$ traversing the CRAC channel compared with Ca^{2+} (measured at 2 mM external [Ca^{2+}]). External Ca^{2+} ions in the micromolar range blocked Na$^+$ current through CRAC channels. In Fig. 3 C, with a single stably open CRAC channel, buffering extracellular Ca^{2+} to 50 μM produced burst-like ("flickering") block and unblock events at −120 mV. Ca^{2+} block reduced the mean open time to <1 ms ($n = 3$), while closed times did not change significantly. The rapid blocking events reflect Ca^{2+} entry into the open channel. Fig. 3 D shows that CRAC channels in resting and activated T cells exhibit identical sensitivity to block by Ca^{2+}. The voltage dependence of block was quantitatively assessed through normalization of I–V curves in the presence and absence of external Ca^{2+} (Fig. 3 E). This procedure revealed that Ca^{2+} block is relieved at either strongly hyperpolarized or depolarized potentials. Na$^+$ currents inactivated if Mg^{2+} (3.6 mM) was present internally (Fig. 3 F). Although Na$^+$ permeates readily in the absence of external divalent ions, NMDG$^+$ did not carry measurable inward current ($n = 8$, not shown). We conclude that the permeation properties and divalent block of
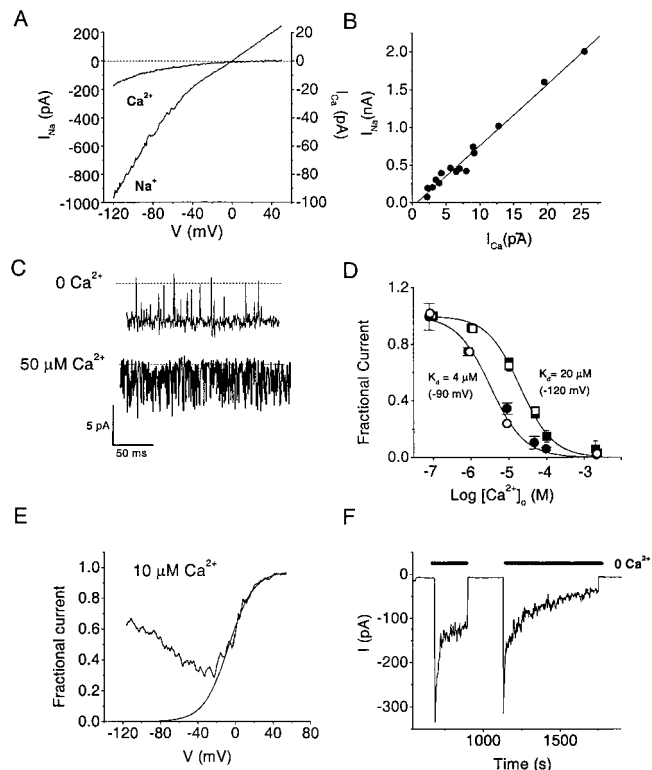
Figure 3. Ionic selectivity, rectification, and divalent block of CRAC channels in human T cells. (A) Na$^+$ and Ca^{2+} currents recorded during a voltage ramp from −120 mV to 50 mV in the absence and presence of 2 mM extracellular Ca^{2+} in an activated T cell. Note the 10-fold difference in scales for I_{Na} and I_{Ca}. External solutions were changed rapidly between Ca^{2+}-free and Ca^{2+}-containing external solutions. (B) Ratio of Na$^+$ to Ca^{2+} current. Na$^+$ current amplitudes measured immediately after application of Ca^{2+}-free solution plotted against Ca^{2+} current amplitude (2 mM external Ca^{2+}). Each point was obtained from an individual PHA-activated cell ($n = 14$) from different donors. The straight line is a linear regression fit with a slope factor of 81.4 ± 2.4 and a correlation coefficient of 0.99. (C) Example of single channel currents recorded at −120 mV from a resting T cell. Top trace recorded in Ca^{2+}-free external solution (10 mM HEDTA, no Ca^{2+} added). Bottom trace recorded after application of 50 μM Ca^{2+} external solution. (D) External Ca^{2+} blocks Na$^+$ current through CRAC channels in resting and activated T cells. Currents at different external Ca^{2+} concentrations were normalized to the current in Ca^{2+}-free external solution. Averaged data from several resting (open symbols) and activated (closed symbols) T cells ($n = 4$–11 cells), fitted with the equation: Fractional Current = $1 / (1 + [Ca^{2+}]_o / K_d)$. Apparent K_d values were 4 μM and 20 μM at −90 mV and −120 mV, respectively. (E) Voltage dependence of Ca^{2+} block. I–V curves recorded in the presence and absence of 10 μM external Ca^{2+} were divided point by point and fitted with the Boltzmann equation: Fractional Current = $1 / \{1 + \exp[(V_h - V) / k]\}$, with $V_h = -7.3$ mV and $k = 13.3$ mV. The steepness factor k is equivalent to movement of a single Ca^{2+} ion 93% of the distance from the outside across the electric field of the membrane to the blocking site within the channel. (F) Ca^{2+} and Na$^+$ currents recorded at −120 mV from a cell dialyzed with 3.6 mM Mg^{2+}. External solution containing 2 mM Ca^{2+} was exchanged with Ca^{2+}-free HEDTA-containing solution as indicated. Note the reversible inactivation of Na$^+$ current.

Table I. CRAC Channel Properties in Resting and Activated Human T Lymphocytes and in Jurkat T Cells

Property	Resting T cells	Activated T cells	Jurkat T cells*
Activation by passive store depletion	Yes	Yes	Yes
IP_3 accelerates activation	Yes	ND	Yes
Single channel Na^+ conductance	41 pS	41 pS	38–40 pS
Open probability (-120 mV)	>0.95	>0.95	>0.94
Ratio of Na^+ to Ca^{2+} current	ND	81.4 ± 2.4 (2 mM Ca^{2+})	27 (20 mM Ca^{2+})
External Ca^{2+} block (-90 mV)	$K_d = 4$ μM	$K_d = 4$ μM	$K_d = 5$ μM
Mg^{2+}-dependent inactivation	Yes	Yes	Yes
Permeability to $NMDG^+$	<0.01	<0.01	<0.01

*Data on Jurkat T cells from Lepple-Wienhues and Cahalan, 1996; Kerschaum and Cahalan, 1998, 1999.

CRAC channels in human T cells are indistinguishable from those described previously in Jurkat T cells (Table I).

Single Channel Kinetics

Resting T cells were favorable for detailed kinetic analysis of single CRAC channels. Single channel recordings during voltage ramps (Fig. 4 A) and continuous recordings at various potentials (Fig. 4 B) suggested that the lifetimes of both open and closed channel states increase upon membrane depolarization, resulting in fewer event transitions. Single channel closed times (τ_c) were consistently <1 ms at -120 mV in all cells tested, and most cells had open times (τ_o) averaging 11.2 ± 0.9 ms, ($n = 11$). Some channels exhibited longer channel open lifetimes ($\tau_o \sim 40$ ms, $n = 9$), and, less frequently, channels with a flickery gating mode were also observed; here we restrict our analysis to the most commonly observed channel behavior. Fig. 4 C shows histograms of closed and open times for a single channel at two potentials. A single exponential function provides an adequate fit to the lifetime distributions, consistent with a simple two-state channel gating scheme with voltage-dependent rate constants connecting a closed state C and an open state O, C↔O. Membrane depolarization from -120 to -20 mV increased both mean closed and open lifetimes (Fig. 4 D). Exponential functions describe the voltage dependence of both open and closed channel lifetimes. The measured increases in τ_o and τ_c predict a weak voltage dependence of P_o from the equation $P_o = \tau_o/(\tau_o+\tau_c)$. Computed values of P_o determined from lifetime measurements are in excellent agreement with direct measurements of P_o obtained by integrating single channel traces (Fig. 4 E). Although not strongly voltage-dependent, the gating process of CRAC channels would contribute to the channel's inward rectification. I–V relationships of single channel Na^+ current obtained during voltage ramps (Fig. 4 A) or from unitary currents at different potentials (Fig. 4 E) exhibited weak inward rectification, a reversal potential near 0 mV, a chord conductance of 41 pS at -120 mV, and a calculated slope conductance of 55 pS between -120 mV and -80 mV.

Upregulated CRAC Channel Expression and Capacitative Ca^{2+} Influx in Activated T Cells

Properties of single CRAC channels were identical in resting and activated T cells, but the number of CRAC channels increased substantially following treatment with PHA to induce T cell activati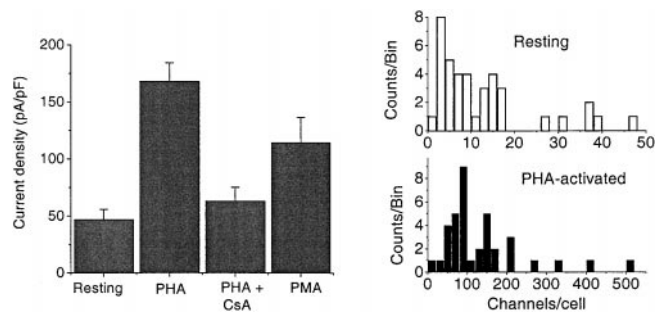on. We confirmed that this treatment also activated IL-2 production by flow cytometric analysis of fixed and permeabilized T cells (data not shown). To evaluate the number and surface density of CRAC channels, peak currents were normalized to membrane capacitance (C_m) in cells selected from resting and PHA-treated T cell populations. Measurements from 15 different donors were combined. Capacitance values were 1.7 ± 0.1 pF in 43 resting T cells and 3.6 ± 0.2 pF in 44 PHA-activated T cells. CRAC channel current density in PHA-treated T cells increased by a factor of four compared with resting T cells (Fig. 5 A). The number of channels per cell increased from 14.9 ± 2.4 ($n = 40$), in resting T cells, to 136.0 ± 19.2 ($n = 37$), in activated T cells (Fig. 5 B). CsA (1 μM) substantially inhibited this increase in functional CRAC channel expression, while also inhibiting PHA-stimulated cell enlargement ($C_m = 2.3 \pm 0.3$ pF, $n = 9$), cell proliferation assessed by uptake of tritiated thymidine (90% block), and IL-2 production (90% block). At lower concentration (100 nM), CsA was less effective in blocking IL-2 production and CRAC channel upregulation. Acute application of PHA or CsA during whole-cell recording had no effect on the amplitude of monovalent CRAC current ($n = 4$, data not shown). These data demonstrate that PHA stimulation to induce T cell activation increases functional expression of CRAC channels. Pretreatment of resting T cells with the phorbol ester PMA (40 nM for 2–4 d) to stimulate PKC-dependent pathways also increased the CRAC channel current density (Fig. 5 A) and the average number of channels per cell (63.6 ± 13.0, $n = 12$), while causing moderate cell enlargement with C_m values averaging 2.8 ± 0.2 pF in the cells selected for recording.

To confirm that upregulated expression of CRAC channels produces larger Ca^{2+} influx upon re-stimulation of intact T cells, we measured the rate of capacitative Ca^{2+} influx in resting and activated T cells using Tg to deplete intracellular Ca^{2+} stores. Fig. 6 A shows averaged $[Ca^{2+}]_i$ traces upon removal of external Ca^{2+}, application of Tg, and reintroduction of external Ca^{2+}; for these experiments, extracellular $[Ca^{2+}]$ was reduced to 300 μM so that the upstroke of the $[Ca^{2+}]_i$ signal could be resolved clearly. $[Ca^{2+}]_i$ signaling in PHA-activated T cells was enhanced, relative to resting T cells, in three respects. First, Tg-induced release from intracellular Ca^{2+} stores in the absence of external Ca^{2+} was increased, from a release transient peaking at 190 ± 2.7 nM ($n = 320$) in resting T cells to 375 ± 16.5 nM ($n = 163$) in activated T cells, suggesting an increased capacity of intracellular Ca^{2+} stores in acti-
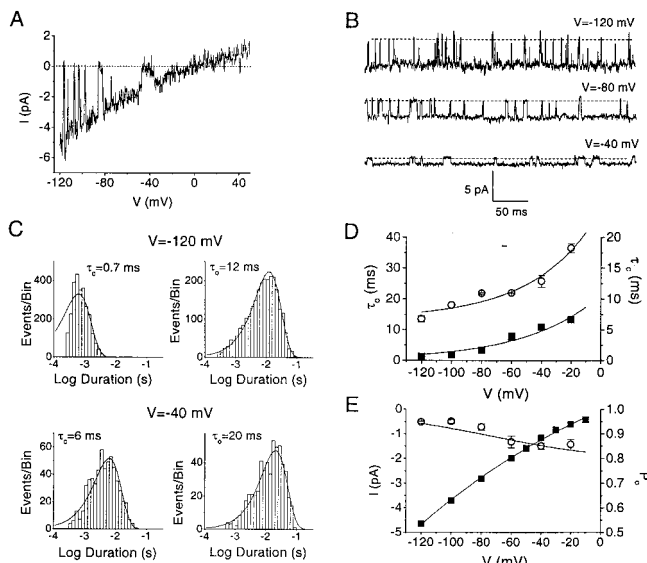
Figure 4. Voltage-dependent properties of single channel currents in resting T cells. (A) Single channel activity during a voltage ramp from −120 to 50 mV. Note the very brief transitions that occur between –120 and –80 mV and longer transitions at more depolarized potentials. (B) Single channel currents recorded at −120, −80, and −40 mV. Again, note that depolarization promotes longer open and closed events. (C) Distributions of open (τ_o) and closed (τ_c) times at −120 and −40 mV. For single channel analysis, traces with stable opening of only one channel were selected. The kinetics of transitions between the open and closed levels were idealized by fitting manually controlled cursors to the two levels and setting a discriminator at 50% of the current between levels. Time histograms computed from a minimum of 60 intervals. Histograms of open and closed event durations were fitted by single Gaussian distributions; two or more components did not provide a significantly better fit. Same cell as in B. (D) Voltage dependence of mean open (τ_o, ○) and mean closed (τ_c, ■) times ($n = 4$). Values of τ_o and τ_c for individual cells were calculated by fitting duration histograms with a single Gaussian function, as described in C. Data are fitted with a single exponential function with a steepness factor $k = 35$ mV for open times and 50 mV for closed times. (E) Single channel current amplitudes (■) and open probabilities (P_o, ○) at varying potentials. Averages from four cells are shown; if not shown, standard error bars are smaller than symbol size. The smooth curve through P_o data was obtained from exponential fits of τ_c and τ_o (smooth lines on D) according to equation $P_o = \tau_o/(\tau_o + \tau_c)$.
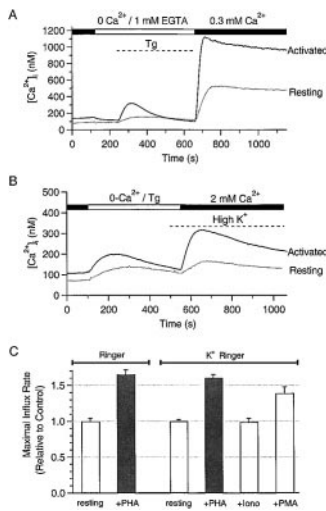

Figure 5. PHA induces functional upregulation of CRAC channels in human T cells. (A) Average CRAC channel Na^{+} current densities in resting, PHA-activated, PHA + CsA-treated, and PMA-treated T cells. Resting T cells were maintained in culture for 24–72 h ($n = 40$). Activated T cells were incubated with PHA for 48–96 h ($n = 37$). Combined data are presented from cells incubated with PHA + CsA for 75 and 96 h ($n = 9$). PMA-treated cells were incubated with 40 nM PMA for 48–96 h ($n = 12$). Between 48 and 96 h, there was no statistically significant difference in CRAC channel expression. Average current densities in resting and PHA + CsA-treated cells are significantly different than those in PHA-activated or PMA-treated T cells (Student's *t* test, $P < 0.001$). (B) Distributions of the number of CRAC channels per cell in resting (top) and PHA-activated (bottom) cell populations. Note the difference in horizontal scales. Maximal currents were divided by the amplitude of single channel current at −120 mV (4.8 pA).

condition, mean influx rates were much lower in K^{+} Ringer than in normal Ringer (9.24 ± 0.25 nM/s in K^{+} Ringer and 24.4 ± 0.9 nM/s in normal Ringer for resting cells). Interestingly, the rate of Ca^{2+} influx in activated cells was still 1.65 ± 0.05 times that observed in resting cells (Fig. 6, B and C). In addition, Ca^{2+}-imaging experiments confirmed that stimulation with PMA alone (40 nM), but not ionomycin alone (200 nM), caused upregulation of CRAC channels. These results are summarized in Fig. 6 C. We conclude that the increased functional expression of CRAC channels results in a significant increase in capacitative Ca^{2+} influx.

Discussion

CRAC Channels in Human T Lymphocytes

Store-operated Ca^{2+} channels play important roles in the regulation of diverse cellular functions in a wide variety of cells. A highly Ca^{2+}-selective type of store-operated channel, the CRAC channel, was originally described in Jurkat T cells, mast cells, and the related RBL cell line (for reviews see Lewis and Cahalan, 1995; Parekh and Penner, 1997; Lewis, 1999). CRAC channels mediate Ca^{2+} influx following receptor stimulation, resulting in [Ca^{2+}]$_i$ signaling that in turn regulates gene transcription and secretion of biologically active molecules in hematopoietic cells (Lewis and Cahalan, 1989; Negulescu et al., 1994; Fanger et al., 1995; Zhang and McCloskey, 1995). Ca^{2+} currents through CRAC channels were reported previously in human T cells and shown to be lacking in a patient suffering from a primary immunodeficiency (Partiseti et al., 1994). However, no data have been available on the single chan-

vated T cells. Second, upon reintroduction of extracellular Ca^{2+}, the rate of rise in [Ca^{2+}]$_i$ was 1.60 ± 0.05 times larger in activated than in resting T cells (Fig. 6, A and C). Third, plateau levels of [Ca^{2+}]$_i$ were also significantly higher in activated T cells (775 ± 22 nM for resting T cells, and 1150 ± 30 nM for activated T cells; Fig. 6 A). Expression levels of both voltage-gated and Ca^{2+}-activated K^{+} channels are known to increase in activated versus resting T cells (Grissmer et al., 1993). To confirm that the observed changes in Ca^{2+} signaling were caused by upregulation of CRAC channels rather than changes in expression of K^{+} channels or membrane potential, we repeated these experiments in the presence of K^{+} Ringer solution (159 mM K^{+}) to null out a possible contribution of the membrane potential to Ca^{2+} influx. As expected for a depolarized

Figure 6. Enhanced capacitative Ca²⁺ entry in activated human T cells. (A) Average time course of changes in $[Ca^{2+}]_i$ upon removal of external Ca²⁺, and consequent reintroduction of 300 μM external Ca²⁺ in resting ($n = 56$, dashed line) and PHA-activated (72 h in PHA; $n = 32$, solid line) T cells. Tg (1 μM) was applied in Ca²⁺-free solution as indicated. Results shown are typical of three to four experiments for each condition with two donors. (B) In this experiment, extracellular solutions were changed to K⁺-Ringer at the end of the store depletion transient, as indicated. Results shown are from 65 activated and 127 resting cells in a typical experiment. (C) The maximal rate of initial Ca²⁺ influx was calculated for each cell by finding the maximal slope between each pair of data points. To prevent bias from donor to donor variability, influx rates for activated cells were normalized to the mean influx rate for resting cells from the same donor on the same day. Influx rates in activated cells and in cells stimulated with PMA alone (but not ionomycin alone) are significantly different from those of resting cells ($P < 0.01$, Mann-Whitney U test). Average maximal influx rates in normal Ringer solution from 320 resting and 163 activated T cells (two donors), and in K⁺ Ringer solution from 452 resting, 382 activated (five donors), 210 ionomycin-treated (two donors), and 72 PMA-treated T cells (one donor) were compiled for this graph.

nel properties or functional expression levels of CRAC channels, or any other Ca²⁺ channels, in normal human T lymphocytes. The use of Na⁺ as the permeant ion permitted CRAC channels to be investigated in Jurkat T cells with single channel resolution (Kerschbaum and Cahalan, 1999). In this study, we demonstrate that Ca²⁺ store depletion in human T cells activates unitary Na⁺ currents through CRAC channels with biophysical properties similar to those described previously in Jurkat T cells (Table I). Single channels with a conductance of 41 pS were visualized during whole-cell recording, using Na⁺ as the permeant ion in divalent-free external solution. External Ca²⁺ in the micromolar range blocked the monovalent current, and at millimolar concentrations exhibited selective permeation with small current magnitudes. The ratio of Na⁺ to Ca²⁺ current was constant from cell to cell, indicating a common channel mechanism. In addition, Na⁺ current exhibited inactivation in the presence of intracellular Mg²⁺. A bulky cation, NMDG⁺, was unable to carry current, as shown previously for CRAC channel currents in Jurkat T cells. These results demonstrate that human T cells express CRAC channels with identical biophysical characteristics to those of Jurkat T cells.

Single Channel Kinetics: Activation and Steady-State Gating

The small number of CRAC channels present in resting T cells provided increased observation time for detailed ki-

netic investigation of single channel properties, compared with Jurkat or activated human T cells. During whole-cell recording, CRAC channels first exhibited very short-duration openings that later stabilized to an open state with intrinsic short-closing events. In resting T cells dialyzed with BAPTA to deplete Ca²⁺ stores passively, the lag time before the first channel opening was relatively long (~1 min), suggesting that the latency to the first channel opening event is rate-limited by the number of functional channels, rather than by the rate of BAPTA dialysis or Ca²⁺ store depletion, which should occur more rapidly in smaller resting T cells. Strong intracellular Ca²⁺ buffering, addition of IP₃ to the pipette, or pretreatment of intact cells with Tg activated the same population of channels by depleting Ca²⁺ stores, similar to results for Ca²⁺ current through CRAC channels (Hoth and Penner, 1992; Zweifach and Lewis, 1993). IP₃ significantly reduced the latency to current activation (Fig. 1 E), similar to that described for I_{CRAC} (Parekh et al., 1997). In addition, CRAC channels opened by Tg pretreatment were detected immediately following break in to initiate whole-cell recording. Thus, Na⁺ current through CRAC channels exhibits normal activation kinetics upon depletion of Tg-sensitive intracellular Ca²⁺ stores.

The mechanism of CRAC channel activation upon Ca²⁺ store depletion remains uncertain. Recent evidence on other store-operated Ca²⁺ channels favors a mechanism that involves close physical contact between the store membrane and the surface membrane, with activation resulting either from channel delivery by vesicle fusion (Patterson et al., 1999; Yao et al., 1999), or by conformational coupling between IP₃ receptors in the store and channels in the surface membrane (Kiselyov et al., 1998; Ma et al., 2000). In principle, a channel delivery mechanism might deliver several channels simultaneously upon vesicle fusion. However, as observed previously in Jurkat T cells (Kerschbaum and Cahalan, 1999), CRAC channel current increased in unitary stepwise increments as individual CRAC channels opened. In these experiments, we never observed the simultaneous initial activation of more than one channel. Furthermore, during the period of CRAC channel activation, no consistent changes in C_m were observed in resting or activated T cells; on average, C_m changed by <5%, or <0.1 pF, a value equivalent to <10 μm². Clearly, major changes in membrane area are not associated with the activation of CRAC channels. Thus, our data do not provide support for the vesicle fusion mechanism, although such a mechanism involving vesicles containing no more than a single CRAC channel, in combination with small vesicle size or a mechanism for membrane retrieval, cannot be excluded.

After channel stabilization, the mean open time was 10 ms, and the mean closed time was <1 ms at −120 mV, resulting in a very high P_o value of >0.95. At more depolarized potentials, both mean open and mean closed times increased, and the open probability declined to ~0.85 at −40 mV. Are these channel gating events intrinsic to the channel protein, or might they be the result of ionic block? With external Ca²⁺ in the micromolar range, individual block and unblock events were visualized as a rapid process that significantly reduced mean open times (<1 ms at 50 μM Ca²⁺ at −120 mV). Maximal block was observed

near -40 mV, with relief of block by depolarization indicating a binding site deep within the channel accessed by external Ca^{2+}, and relief of block at hyperpolarized potentials suggesting "punch-through" of bound Ca^{2+} to the inside induced by the strong electric field within the channel. These results suggest the possibility that trace concentrations of external Ca^{2+}, or another polyvalent cation, could produce channel block at moderate membrane potentials, perhaps even in the presence of a strong Ca^{2+} chelator like HEDTA, and account for channel gating. However, in this case, we would expect a decrease in mean open time at the potentials where divalent block is maximal. Instead, in the absence of external Ca^{2+} and with 10 mM HEDTA outside, both open and closed channel lifetimes increased monotonically with depolarization, with P_o remaining high over a broad potential range, suggesting that inward rectification is not the result of ionic block. Open and closed channel lifetimes are weakly voltage dependent, but current amplitudes are strongly dependent on voltage because changes in the electrical driving force affect the unitary current amplitude. Thus, voltage is a dominant fast regulatory mechanism controlling the amount of Ca^{2+} entry through open CRAC channels that exhibit weakly voltage-dependent gating.

CRAC Channel Expression and Ca^{2+} Influx Rates in Resting and Activated T Cells

Ca^{2+} influx through CRAC channels underlies $[Ca^{2+}]_i$ signaling in Jurkat T cells, and, by extension, is thought to trigger antigen-induced activation of resting human T cells. Whole-cell recordings with single channel resolution enable the number of CRAC channels per cell to be determined in resting and activated cells. Despite their importance for lymphocyte activation, CRAC channels in resting T cells are expressed at surprisingly low copy number, averaging 15 functional CRAC channels per cell. Is this small number of channels sufficient to account for tracer Ca^{2+} influx measurements and for the rate of rise of $[Ca^{2+}]_i$ during activation? To address this question, we calculated the expected influx of Ca^{2+} under physiological conditions during a stimulus that opens all of the available CRAC channels (Fig. 7). Macroscopic Na^+ currents were consistently ~80-fold larger than Ca^{2+} currents recorded with 2 mM external $[Ca^{2+}]$, leading to an estimated single channel conductance of 0.5 pS at -120 mV for Ca^{2+} current through the CRAC channel with physiological levels of external Ca^{2+}. This estimate is based upon the assumption that the number of open channels remains constant during rapid solution exchange. To calculate Ca^{2+} influx in the range of membrane potentials found normally in intact T cells, we scaled the measured single channel Na^+ current at -60 mV by the factor 80 and converted to flux units. In a cell with 15 activated CRAC channels, the calculated Ca^{2+} influx at a resting membrane potential of -60 mV would be 1.9 amol/s, sufficient to account for previous measurements of ^{45}Ca uptake in resting T cells upon mitogen activation, which ranged from 0.4 to 2.2 amol/s (Metcalfe et al., 1980; Hesketh et al., 1983). Can this amount of Ca^{2+} influx produce the upstroke of the $[Ca^{2+}]_i$ signal? The expected rise in $[Ca^{2+}]_i$ due to Ca^{2+} influx depends upon cell volume and buffer capacity. Cell volume was estimated to

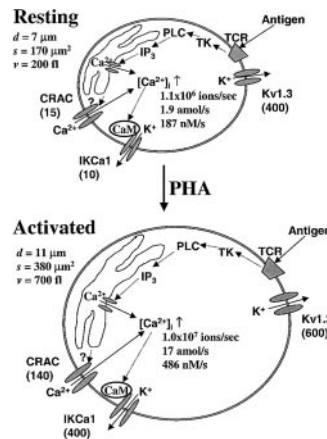*Figure 7.* Channel expression and calculated Ca^{2+} influx in resting and activated T lymphocytes. The two cells depicted in cartoon form represent typical resting (top) and activated (bottom) T cells. Diameters (*d*), surface areas (*s*), and volumes (*v*) are representative of cells selected for recording. Within each cell, a signal transduction pathway leads from antigen binding to the TCR, activating tyrosine kinases (TK), phosphorylating phospholipase C (PLC), generating IP_3, and releasing Ca^{2+} from the store. Ca^{2+} influx through CRAC channels is activated by the depletion of Ca^{2+} from the IP_3-sensitive intracellular Ca^{2+} store via an unknown mechanism. Functional expression levels are represented by the average number of channels per cell (in parentheses), for three channel types: voltage-gated K^+ channels encoded by *Kv1.3* (DeCoursey et al., 1984; Deutsch et al., 1986), Ca^{2+}-activated K^+ channels encoded by *IKCa1* together with preassociated calmodulin (CaM) (Grissmer et al., 1993; Fanger et al., 1999; Ghanshani et al., 2000), and CRAC channels (this paper, Fig. 5 B). The calculated Ca^{2+} influx (ions/sec and amol/s) is based upon the number of CRAC channels per cell, the measured single CRAC channel conductance for Na^+, the measured ratio of I_{Ca}/I_{Na}, and an assumed membrane potential of -60 mV. The maximal rate of $[Ca^{2+}]_i$ increase (d$[Ca^{2+}]_i$/dt in nM/s), resulting from the Ca^{2+} influx with external Ca^{2+} of 2 mM is based upon the estimated cell volume and the buffer capacity.

be 200 fl (200×10^{-15} liter) from measured values of membrane capacitance. An endogenous Ca^{2+} buffer was assumed to capture 99% of the Ca^{2+} entering the cell (Neher and Augustine, 1992; Neher, 1995). Given these estimates and scaling external $[Ca^{2+}]$ to 0.3 mM for comparison with our measurements, the Ca^{2+} influx through 15 CRAC channels would produce a rise in $[Ca^{2+}]_i$ of 28 nM/s in resting T cells, in close agreement with direct measurements of capacitative Ca^{2+} influx in resting T cells averaging 24.4 ± 0.9 nM/s. Thus, despite their small number, CRAC channels would carry sufficient Ca^{2+} into resting T cells to account for measured tracer Ca^{2+} influx and the rates of rise of $[Ca^{2+}]_i$.

CRAC channel properties were identical in resting and activated T cells. However, activated T cells expressed substantially more functional channels, averaging 136 CRAC channels per cell. This functional upregulation of CRAC channels in human T lymphocytes paralleled the growth of small lymphocytes to T cell blasts. In our experiments, average membrane capacitance values increased from 1.7 pF in resting T cells to 3.6 pF in activated T cells, indicating an increase in volume to 700 fl. As calculated for resting cells above, the expected maximal rise in $[Ca^{2+}]_i$ due to Ca^{2+} entry via CRAC channels in a typical activated T cell was 73 nM/s, roughly twofold larger than, but still in reasonable agreement with, the average rate of

43.7 $\pm$ 1.6 nM/s obtained by direct measurements of $[Ca^{2+}]_i$ rise induced by capacitative Ca^{2+} influx. A higher Ca^{2+} buffering capacity or increased pump activity in activated T cells may account for the difference between those numbers. Thus, the increase in number of functional channels in activated T cells not only compensates for cell enlargement but also enhances Ca^{2+} signaling in activated T cells.

Significance of Channel Upregulation for T Cell Function

During T cell activation, numerous transcription factors are activated, resulting in changes in the expression level of many different genes (Lanzavecchia and Sallusto, 2000). Some gene products, such as IL-2 and other secreted lymphokines, help to carry out the effector functions of T cells, and others, such as the Ca^{2+}-activated K^+ (K_{Ca}) channel encoded by *IKCa1*, help to augment $[Ca^{2+}]_i$ signaling and activation responses upon future restimulation. Increased expression of IL-2 is regulated by several transcription factors, but can be inhibited by the immunosuppressive drug CsA at doses that prevent dephosphorylation and nuclear translocation of the transcription factor NF-AT by the phosphatase calcineurin (Rao et al., 1997; Crabtree, 1999). In contrast, enhanced expression of K_{Ca} channels is transcriptionally regulated by AP-1 and Ikaros-2 sites in the promoter region and is independent of NF-AT, since enhanced expression can be stimulated by PMA alone and is unaffected either by CsA treatment or by deletion of an NF-AT-binding element in the promoter region of the *IKCa1* gene (Ghanshani et al., 2000). The increased number of CRAC channels in activated T cells may also result from transcriptional upregulation of the unknown gene or genes that encode CRAC channels. Both CRAC and K_{Ca} channel expression increase greatly in T cells stimulated for at least 24 h with PHA or PMA alone, but not with ionomycin alone (Figs. 5–7), suggesting a similar mechanism. In addition, CsA, at a concentration reported to block calcineurin-mediated nuclear translocation of NF-AT (Rao et al., 1997), did not inhibit CRAC channel upregulation. However, PHA-induced IL-2 secretion, T cell proliferation, and upregulation of CRAC channels were inhibited by CsA at a concentration of 1 μM, a level that may have nonspecific effects. Thus, a possible direct role of calcineurin and NF-AT in CRAC channel upregulation requires further investigation. A detailed understanding of the mechanism awaits molecular identification of the CRAC channel.

Two levels of positive feedback involving CRAC and K_{Ca} channels augment $[Ca^{2+}]_i$ signaling, as suggested by Fig. 7. Before TCR engagement, $[Ca^{2+}]_i$ is low ($\sim$100 nM), CRAC and K_{Ca} channels are closed, and the resting membrane potential is maintained by voltage-gated Kv1.3 channels. After TCR engagement, $[Ca^{2+}]_i$ begins to rise, initially due to IP_3-induced release of Ca^{2+}. The depletion of IP_3-sensitive Ca^{2+} stores opens CRAC channels, further elevating $[Ca^{2+}]_i$. As soon as $[Ca^{2+}]_i$ reaches 200–300 nM, K_{Ca} channels begin to open, hyperpolarizing the membrane and thereby increasing Ca^{2+} influx through CRAC channels, in turn augmenting the rise in $[Ca^{2+}]_i$ and opening the remaining K_{Ca} channels. Thus, rapid positive feedback among $[Ca^{2+}]_i$, K_{Ca} channels, and CRAC channels contributes to the upstroke of the Ca^{2+} signal. In addition, slow positive feedback involving changes in gene expression is initiated by the rise in $[Ca^{2+}]_i$, along with other signaling pathways inside the cell. Activated T cells exhibit enhanced Ca^{2+} signaling in response to either TCR engagement or Tg stimulation (Hess et al., 1993; Verheugen et al., 1997) (Fig. 6). Increased expression of CRAC channels in activated T cells occurs in parallel with a comparable increase in expression of Ca^{2+}-activated K^+ channels encoded by *IKCa1* (Grissmer et al., 1993; Ghanshani et al., 2000). Relative to resting T cells, Tg-induced Ca^{2+} influx is augmented in activated T cells by the same amount in normal Ringer and in K^+ Ringer (1.65 $\pm$ 0.06-fold upregulation in normal Ringer vs. 1.60 $\pm$ 0.05-fold upregulation in K^+ Ringer). This implies that upregulation of CRAC channels augments Ca^{2+} signaling, and that parallel K_{Ca} channel upregulation is adequate to provide the necessary driving force and to compensate for the increase in cell size. Without accompanying K_{Ca} channel upregulation, Ca^{2+} influx through the increased number of CRAC channels would depolarize the membrane, causing Ca^{2+} influx to be self-limiting.

Amplification of the Ca^{2+} signal may be responsible for increased sensitivity to TCR stimulation observed previously in secondary T cell activation (Manger et al., 1985; Byrne et al., 1988). In addition, upregulation of Ca^{2+} influx through CRAC channels may sustain mitogenesis. The number of CRAC channels in activated T cells ($\sim$140 per cell) is close to that in proliferating Jurkat T cells (100–400 per cell), suggesting a requirement for larger numbers of CRAC channels for clonal expansion. Sustained $[Ca^{2+}]_i$ elevation is required for calcineurin-dependent translocation of NF-AT into the nucleus, resulting in activation of NF-AT–dependent transcription of lymphokines, and presumably other immune response genes (Rao et al., 1997; Crabtree, 1999). Therefore, functional upregulation of CRAC channels may play a crucial role for continued cell proliferation and more vigorous secondary T cell responses.

References

Byrne, J.A., J.L. Butler, and M.D. Cooper. 1988. Differential activation requirements for virgin and memory T cells. *J. Immunol.* 141:3249–3257.

Crabtree, G.R. 1989. Contingent genetic regulatory events in T lymphocyte activation. *Science.* 243:355–361.

Crabtree, G.R. 1999. Generic signals and specific outcomes: signaling through Ca^{2+}, calcineurin, and NF-AT. *Cell.* 96:611–614.

Crabtree, G.R., and N.A. Clipstone. 1994. Signal transmission between the plasma membrane and nucleus of T lymphocytes. *Ann. Rev. Biochem.* 63:1045–1083.

DeCoursey, T.E., K.G. Chandy, S. Gupta, and M.D. Cahalan. 1984. Voltage-gated K^+ channels in human T lymphocytes: a role in mitogenesis? *Nature.* 307:465–468.

Deutsch, C., D. Krause, and S.C. Lee. 1986. Voltage-gated potassium conductance in human T lymphocytes stimulated with phorbol ester. *J. Physiol. (Lond.).* 372:405–423.

Dolmetsch, R.E., and R.S. Lewis. 1994. Signaling between intracellular Ca21

stores and depletion-activated Ca²⁺ channels generates [Ca²⁺]ᵢ oscillations in T lymphocytes. *J. Gen. Physiol.* 103:365–388.

Donnadieu, E., D. Cefai, Y.P. Tan, G. Paresys, and G. Bismuth. 1992. Imaging early steps of human T cell activation by antigen-presenting cells. *J. Immunol.* 148:2643–2653.

Fanger, C.M., M. Hoth, G.R. Crabtree, and R.S. Lewis. 1995. Characterization of T cell mutants with defects in capacitative calcium entry: genetic evidence for the physiological roles of CRAC channels. *J. Cell Biol.* 131:655–667.

Fanger, C.M., S. Ghanshani, N.J. Logsdon, H. Rauer, K. Kalman, J. Zhou, K. Beckingham, K.G. Chandy, M.D. Cahalan, and J. Aiyar. 1999. Calmodulin mediates calcium-dependent activation of the intermediate conductance K_Ca channel, *IKCa1*. *J. Biol. Chem.* 274:5746–5754.

Fanger, C.M., A.L. Neben, and M.D. Cahalan. 2000. Differential Ca²⁺ influx, K_Ca channel activity and Ca²⁺ clearance distinguish Th1 and Th2 lymphocytes. *J. Immunol.* 164:1153–1160.

Ghanshani, S., H. Wulff, M.J. Miller, H. Rohm, A. Neben, G.A. Gutman, M.D. Cahalan, and K.G. Chandy. 2000. Up-regulation of the *IKCa1* potassium channel during T-cell activation: molecular mechanism and functional consequences. *J. Biol. Chem.* 10.1074/jbc.m003941200.

Grissmer, S., A.N. Nguyen, and M.D. Cahalan. 1993. Calcium activated potassium channels in resting and activated human T lymphocytes. *J. Gen. Physiol.* 102:601–630.

Hesketh, T.R., G.A. Smith, J.P. Moore, M.V. Taylor, and J.C. Metcalfe. 1983. Free cytoplasmic calcium concentration and the mitogenic stimulation of lymphocytes. *J. Biol. Chem.* 258:4876–4882.

Hess, S.D., M. Oortgiesen, and M.D. Cahalan. 1993. Calcium oscillations in human T and natural killer cells depend upon membrane potential and calcium influx. *J. Immunol.* 150:2620–2633.

Hoth, M., and R. Penner. 1992. Depletion of intracellular calcium stores activates a calcium current in mast cells. *Nature.* 355:353–356.

Hoth, M., and R. Penner. 1993. Calcium release-activated calcium current in rat mast cells. *J. Physiol.* 465:359–386.

Kerschbaum, H.H., and M.D. Cahalan. 1998. Monovalent permeability, rectification, and ionic block of store-operated calcium channels in Jurkat T lymphocytes. *J. Gen. Physiol.* 111:521–537.

Kerschbaum, H.H., and M.D. Cahalan. 1999. Single-channel recording of a store-operated Ca²⁺ channel in Jurkat T lymphocytes. *Science.* 283:836–839.

Kiselyov, K., X. Xu, G. Mozhayeva, T. Kuo, I. Pessah, G. Mignery, X. Zhu, L. Birnbaumer, and S. Muallem. 1998. Functional interaction between InsP3 receptors and store-operated Htrp3 channels. *Nature.* 396:478–482.

Lanzavecchia, A., and F. Sallusto. 2000. From synapses to immunological memory: the role of sustained T cell stimulation. *Curr. Opin. Immunol.* 12:92–98.

Lepple-Wienhues, A., and M.D. Cahalan. 1996. Conductance and permeation of monovalent ions through depletion-activated Ca²⁺ channels (I_CRAC) in Jurkat T cells. *Biophys. J.* 71:787–794.

Lewis, R.S. 1999. Store-operated calcium channels. *Adv. Second Messenger Phosphoprotein Res.* 33:279–307.

Lewis, R.S., and M.D. Cahalan. 1989. Mitogen-induced oscillations of cytosolic Ca²⁺ and transmembrane Ca²⁺ current in human leukemic T cells. *Cell Regul.* 1:99–112.

Lewis, R.S., and M.D. Cahalan. 1995. Potassium and calcium channels in lymphocytes. *Annu. Rev. Immunol.* 13:623–653.

Ma, H.-T., R.L. Patterson, D.B. van Rossum, L. Birnbaumer, K. Mikoshiba, and D.L. Gill. 2000. Requirement of the inositol trisphosphate receptor for activation of store-operated Ca²⁺ channels. *Nature.* 287:1647–1651.

Manger, B., A. Weiss, C. Weyand, J. Goronzy, and J.D. Stobo. 1985. T cell activation: Differences in the signals required for IL 2 production by nonactivated and activated T cells. *J. Immunol.* 135:3669–3673.

Metcalfe, J.C., T. Pozzan, G.A. Smith, and T.R. Hesketh. 1980. A calcium hypothesis for the control of cell growth. *Biochem. Soc. Symposia.* 45:1–26.

Neher, E. 1988. The influence of intracellular calcium concentration on degranulation of dialysed mast cells from rat peritoneum. *J. Physiol.* 395:193–214.

Neher, E. 1995. The use of Fura-2 for estimating Ca buffers and Ca fluxes. *Neuropharmacology.* 34:1423–1442.

Neher, E., and G.J. Augustine. 1992. Calcium gradients and buffers in bovine chromaffin cells. *J. Physiol.* 450:273–304.

Negulescu, P.A., T.B. Krasieva, A. Khan, H.H. Kerschbaum, and M.D. Cahalan. 1996. Polarity of T cell shape, motility and sensitivity to antigen. *Immunity.* 4:421–430.

Negulescu, P.A., N. Shastri, and M.D. Cahalan. 1994. Intracellular calcium dependence of gene expression in single T lymphocytes. *Proc. Natl. Acad. Sci. USA.* 91:2873–2877.

Parekh, A.B., and R. Penner. 1997. Store depletion and calcium influx. *Physiol. Rev.* 77:901–930.

Parekh, A.B., A. Fleig, and R. Penner. 1997. The store-operated calcium current I(CRAC): nonlinear activation by InsP3 and dissociation from calcium release. *Cell.* 89:973–980.

Partiseti, M., F. Le Deist, C. Hivroz, A. Fischer, H. Korn, and D. Choquet. 1994. The calcium current activated by T cell receptor and store depletion in human lymphocytes is absent in a primary immunodeficiency. *J. Biol. Chem.* 269:32327–32335.

Patterson, R.L., D.B. van Rossum, and D.L. Gill. 1999. Store-operated Ca²⁺ entry: evidence for a secretion-like coupling model. *Cell.* 98:487–499.

Rao, A. 1994. NF-ATp: a transcription factor required for the co-ordinate induction of several cytokine genes. *Immunol. Today.* 15:274–281.

Rao, A., C. Luo, and P.G. Hogan. 1997. Transcription factors of the NFAT family: regulation and function. *Ann. Rev. of Immunol.* 15:707–747.

Schreiber, S.L., and G.R. Crabtree. 1992. The mechanism of action of cyclosporin A and FK506. *Immunol. Today.* 13:136–142.

Verheugen, J.A.H., F. Le Deist, V. Devignot, and H. Korn. 1997. Enhancement of calcium signaling and proliferation responses in activated human T lymphocytes. *Cell Calcium.* 21:1–17.

Yao, Y., A.V. Ferrer-Montiel, M. Montal, and R.Y. Tsien. 1999. Activation of store-operated Ca²⁺ current in Xenopus oocytes requires SNAP-25 but not a diffusible messenger. *Cell.* 98:475–485.

Zhang, L., and M.A. McCloskey. 1995. Immunoglobulin E receptor-activated calcium conductance in rat mast cells. *J. Physiol.* 483:59–66.

Zweifach, A., and R.S. Lewis. 1993. Mitogen-regulated Ca²⁺ current of T lymphocytes is activated by depletion of intracellular Ca²⁺ stores. *Proc. Natl. Acad. Sci. USA.* 90:6295–6299.